

# Penetration of Josephson vortices and measurement of the $c$ -axis penetration depth in $\text{Bi}_2\text{Sr}_2\text{CaCu}_2\text{O}_{8+\delta}$ : Interplay of Josephson coupling, surface barrier and defects

H. Enriquez, N. Bontemps

*Laboratoire de Physique de la Matière Condensée, Ecole Normale Supérieure, 24 rue Lhomond, 75231 Paris Cedex 05, France*

A. A. Zhukov, D. V. Shovkun, M. R. Trunin

*Institute of Solid State Physics RAS, 142432 Chernogolovka, Moscow district, Russia*

A. Buzdin, M. Daumens

*Laboratoire de Physique Théorique, Université Bordeaux I, 33405 Talence Cedex, France*

T. Tamegai

*Department of Applied Physics, The University of Tokyo, Hongo, Bunkyo-ku, Tokyo 113-8656, Japan*

The first penetration field  $H_J(T)$  of Josephson vortices is measured through the onset of microwave absorption in the locked state, in slightly overdoped  $\text{Bi}_2\text{Sr}_2\text{CaCu}_2\text{O}_{8+\delta}$  single crystals ( $T_c \approx 84$  K). The magnitude of  $H_J(T)$  is too large to be accounted for by the first thermodynamic critical field  $H_{c1}(T)$ . We discuss the possibility of a Bean-Livingston barrier, also supported by irreversible behavior upon flux exit, and the role of defects, which relates  $H_J(T)$  to the  $c$ -axis penetration depth  $\lambda_c(T)$ . The temperature dependence of the latter, determined by a cavity perturbation technique and a theoretical estimate of the defect-limited penetration field are used to deduce from  $H_J(T)$  the absolute value of  $\lambda_c(0) = (35 \pm 15)$   $\mu\text{m}$ .

PACS numbers: 47.32Cc, 74.72h, 78.70Gq

## I. INTRODUCTION

The phenomenological Lawrence-Doniach model is generally used to describe a stack of Josephson-coupled superconducting layers<sup>1-3</sup>. This interlayer Josephson tunneling has been established experimentally by dc or ac Josephson effect experiments in numerous high- $T_c$  superconductors<sup>4</sup> and is proposed as a candidate mechanism for superconductivity<sup>5</sup>. Such discrete layered structures have some striking incidence on many properties:

i) Josephson vortices appear for field parallel to the layers, and in case their penetration in this quasi-2D system is impeded by a surface barrier<sup>6</sup>, the penetration field, henceforward noted  $H_e^{2D}(T)$ , is simply inversely proportional to the  $c$ -axis penetration depth  $\lambda_c(T)$ <sup>7</sup>, unlike isotropic superconductors (where it is of the order of the thermodynamic critical field). The occurrence of such a barrier was discussed mostly in the framework of low-field magnetization measurements performed in fields parallel to the layers in  $\text{NdCeCuO}_8$ , Tl-2201<sup>9</sup> and Bi-2212<sup>10</sup>. The quantitative estimates of  $\lambda_c(T)$  deduced from these data were however disputed<sup>11</sup>.

ii)  $\lambda_c(T)$  is directly related to the critical current density between the layers,  $J_0(T)$ , and is inversely proportional to the Josephson plasma frequency  $\omega_{ps}$ <sup>12,13</sup>. Both quantities ought to be discussed within the same theoretical background<sup>15,16</sup>. Direct determination of the plasma frequency was performed through infrared reflectivity measurements in  $\text{La}_{2-x}\text{Sr}_x\text{CuO}_4$ <sup>17</sup>,  $\text{YBa}_2\text{Cu}_3\text{O}_{6+\delta}$ <sup>18</sup>, Tl-2212 or Tl-2201<sup>19</sup> and from microwave absorption measurements in underdoped Bi-2212 and Bi-2201<sup>20</sup>. A large

body of literature reported a sharp microwave absorption line in presence of a static field applied parallel to the  $c$ -axis<sup>21,22</sup>. This absorption line was assigned to Josephson plasma resonance, whose frequency is modified by the field-dependent interlayer phase coherence<sup>12,23</sup>. However, this interpretation is still controversial<sup>24</sup>. Although the geometry of the experiments reported here is different (the external field is parallel to the  $ab$  planes), the specific field dependence of  $\lambda_c$  or  $\omega_{ps}$  may be involved, as discussed elsewhere<sup>14-16</sup>.

Therefore, an independent measurement of the absolute value of  $\lambda_c$  (in zero applied field) is of interest. To date, all the above mentioned properties have been studied separately. It is the aim of this paper to bring together two different microwave measurements in order to obtain the absolute value of  $\lambda_c(T)$ : i) the first penetration field of Josephson vortices is measured and shown to be related to  $\lambda_c(T)$ , ii) a cavity perturbation technique<sup>25</sup> is used to determine the temperature variation of  $\Delta\lambda_{ab}(T)$  and  $\Delta\lambda_c(T)$ <sup>26</sup>.

In the present paper, we focus mainly on the investigation of the penetration of Josephson vortices through surface resistance measurements at high frequency (10 GHz) in Bi-2212<sup>27</sup>. The onset of microwave absorption allows to determine the penetration field  $H_J(T)$  of Josephson vortices at different temperatures. The magnitude of  $H_J(T)$  and the irreversible behavior of the dissipation with respect to flux entry and flux exit point at first sight toward a Bean-Livingston surface barrier impeding the penetration of Josephson vortices. However, a closer quantitative investigation, which includes the experimental determination of the variation  $\Delta\lambda_c(T)$  of the

$c$ -axis penetration depth, and the theoretical calculation of the penetration field in the presence of edge or surface defects, leads us to the conclusion that  $H_J(T)$  is eventually controlled by such surface irregularities. Relying on these theoretical estimates, we deduce from  $H_J(T)$  the absolute value of the  $c$ -axis penetration depth.

## II. EXPERIMENT

Microwave dissipation measurements were performed in various (generally slightly over-doped) BSCCO single crystals shaped into rectangular platelets of approximate size  $a \times b \times c \simeq 2 \times 1 \times 0.03$  mm<sup>3</sup>: sample A,  $T_c = 86$  K, has a transition width  $\Delta T_c \approx 3$  K (as determined from the range over which the microwave absorption drops from normal to superconducting state values), sample B with  $T_c = 84$  K,  $\Delta T_c \approx 3$  K, sample C,  $T_c = 89$  K,  $\Delta T_c \approx 3$  K. Two other similar samples (D and E) were used for checking the onset of microwave dissipation with respect to the surface quality as discussed below. Finally, the temperature dependence of the penetration depth was measured in a set of similar samples by a cavity perturbation technique at 10 GHz and ac-susceptibility at 100 kHz. The details of these measurements will be discussed elsewhere<sup>26</sup> while here we shall only make use of the temperature variations of  $\Delta\lambda_{ab}(T)$  and  $\Delta\lambda_c(T)$ . An example of the temperature dependence of the surface resistance  $R_s(T)$  in the  $ab$ -plane of slightly overdoped ( $T_c = 84$  K) BSCCO single crystal is shown in Fig. 1. The extrapolation of this curve to  $T = 0$  (inset of Fig. 1) yields estimate  $R_{res} \approx 110 \mu\Omega$ , which is, to the best of our knowledge, the lowest value ever obtained in BSCCO single crystals at 10 GHz. The inset of Fig. 1 displays also the linear change with temperature ( $T < 50$  K) of  $\Delta\lambda_{ab}(T) = \lambda_{ab}(T) - \lambda_{ab}(5K)$ . This linear variation at low  $T$  was previously observed in optimally doped<sup>28-30</sup> and slightly overdoped<sup>30</sup> BSCCO single crystals. Both of the above mentioned parameters of the sample suggest that the quality of the cuprate planes is fairly high. We note that the slope of  $\Delta\lambda_{ab}(T)$  in the inset of Fig. 1 is fairly large ( $\approx 25$  Å/K). It could be a consequence of doping<sup>30,31</sup> with respect to optimally doped crystals<sup>28,29</sup>.

All samples from different batches exhibit very similar properties as far as the magnitude and temperature dependence of the field penetration is concerned, so that experimental results are only displayed for sample A.  $\Delta\lambda_c(T)$  differs among samples with different  $T_c$ . We shall only make use of the data on the samples with the same  $T_c$  ( $\pm 1$  K).

The experimental set-up was described elsewhere<sup>32</sup>. It is used to measure the microwave losses as a function of the applied magnetic field (0-100 Oe) and temperature (50-90 K, measurements at temperatures lower than 45 K are hindered by the increasing noise of the set-up).

The microwave field  $\mathbf{h}_1$  lies within the  $ab$ -plane, so that the induced microwave currents flow both within the  $ab$ -

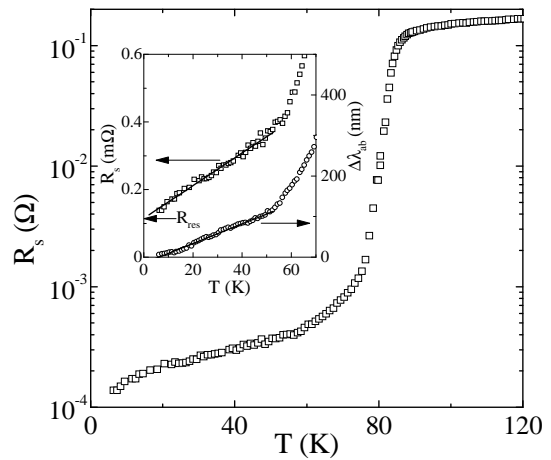


FIG. 1. Surface resistance  $R_s(T)$  in the  $ab$ -plane of slightly overdoped BSCCO single crystal. The inset shows the low temperature behavior of  $R_s(T)$  and of the penetration depth  $\Delta\lambda_{ab}(T)$ .

plane and along the crystallographic  $c$ -axis. The static magnetic field  $\mathbf{H}$  is applied in the  $ab$ -plane perpendicular to the microwave field. A computer-controlled goniometer allows to select its orientation  $\theta$  with respect to the  $ab$ -plane. To locate the  $\theta = 0$  position, we take advantage of the lock-in transition evidenced earlier<sup>32</sup>. The set-up measures the variation of the power dissipated in the cavity as the magnetic field is swept at fixed temperature, hence yields the field induced imaginary part  $\chi''(H)$  of the macroscopic susceptibility<sup>33</sup> (as long as the dissipation is ohmic, the so-called linear regime). This latter point has been checked for all the data shown henceforward.

## III. RESULTS

Figure 2 displays the change of dissipation  $\chi''(H) - \chi''(0)$ , starting from zero field (within  $\pm 0.1$  Oe) measured in sample A for various orientations of the applied field close to the  $ab$ -plane:  $0^\circ \leq \theta \leq 3^\circ$  (only the  $0^\circ$  and  $2^\circ$  are displayed in Fig. 2) and in a low-field range:  $0 \leq H \leq 25$  Oe, at three typical temperatures ( $T = 78$  K, 65 K, 50 K).

After each field sweep, the sample was warmed through  $T_c$  and then cooled again in zero field, in order to avoid any possible vortex pinning when studying the penetration starting from zero field. The dissipation of Josephson vortices is characterized by the fact that it does not depend on the angle (Fig. 2), as long as these vortices remain locked. According to our previous study, the dissipation regime displayed in Fig. 2 comes only from locked Josephson vortices<sup>32</sup> and holds up to  $\sim 30$  Oe.

As the field increases, an onset in the dissipation occurs at a temperature-dependent field  $H_J(T)$  (Fig. 2), which we associate to Josephson vortices entering the sample. Interestingly, above  $H_J(T)$ , the microwave ab-

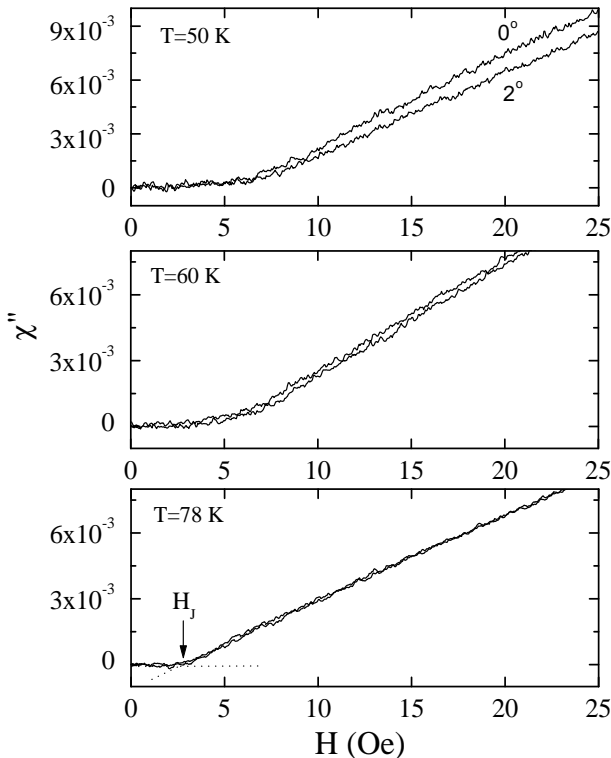


FIG. 2. Dissipation as a function of the applied field at 3 temperatures, for 2 orientations ( $0^\circ$  and  $2^\circ$ ) of the applied field with respect to the  $ab$ -plane. The onset of dissipation, indicated by the arrow, occurs at the penetration field  $H_J(T)$ .

sorption behaves linearly with field, with a very good accuracy, from typically 10 Oe up to 25 Oe. This appears consistent with a flux-flow mechanism driven by  $c$ -axis currents, where the flux-flow resistivity is linear with applied field. We therefore identify  $H_J(T)$  to the first penetration field of Josephson vortices. In this work, unlike in Ref.<sup>27</sup>, we have averaged the data over the field orientations from  $0^\circ$  to  $3^\circ$ , in an attempt to improve the accuracy of the determination. As in Ref.<sup>27</sup>, we choose to define  $H_J(T)$  as the field value where the microwave absorption exceeds the experimental accuracy ( $2 \cdot 10^{-4}$ ). The field thus determined is plotted in Fig. 3. The error bars take into account both the noise and the estimated drift of the signal with time<sup>34</sup>.

#### IV. DISCUSSION

Whether  $H_J(T)$  may be identified to the thermodynamic lower critical field  $H_{c1}$  was previously discussed<sup>27,32</sup>. For Josephson vortices  $H_{c1}$  writes<sup>3</sup>:

$$H_{c1}(T) = \frac{\phi_0}{4\pi\lambda_{ab}(T)\lambda_c(T)} [\ln \lambda_{ab}(T)/d + 1.12] \quad (1)$$

In our early work<sup>32</sup>, we had not yet studied the temperature dependence of  $H_J(T)$  and we had not observed the

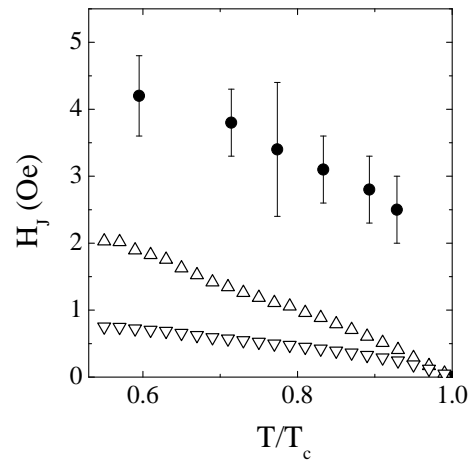


FIG. 3. Plot of  $H_J(T)$  (full circles). Up (down) triangles display estimates of  $H_{c1}(T)$  using  $\lambda_c(0) = 10 \mu\text{m}$  ( $40 \mu\text{m}$ ). The temperature variations  $\Delta\lambda_{ab}(T)$  and  $\Delta\lambda_c(T)$  are taken from our present work (Figs. 1,5).

irreversible behavior of the dissipation upon flux entry and flux exit. We had therefore not considered the possibility of a surface barrier. However, in order to reconcile the magnitude of  $H_J(T \ll T_c)$  with the thermodynamic lower critical field, we were compelled to take the lowest possible values for  $\lambda_{ab}(0)$  and  $\lambda_c(0)$ .

We proposed next in Ref.<sup>27</sup> to take more acceptable lower bounds for  $\lambda_{ab}(0)$  and  $\lambda_c(0)$ , together with the experimentally determined temperature variations in order to obtain an upper bound for  $H_{c1}(T)$ . Here, we take  $2100 \text{ \AA}$  as a lower bound for  $\lambda_{ab}(0)$ <sup>29,35</sup>, and  $10 \mu\text{m}$  for  $\lambda_c(0)$ <sup>22,36-43</sup>. We use the temperature dependence for  $\Delta\lambda_{ab}(T)$  (partly shown in the inset of Fig. 1) and  $\Delta\lambda_c(T)$  measured in our previous work<sup>26</sup> (see Fig. 5 below). The corresponding  $H_{c1}(T)$  is plotted in Fig. 3 using the above mentioned values. We have also displayed in Fig. 3  $H_{c1}(T)$  if taking  $\lambda_c(0) = 40 \mu\text{m}$ <sup>26,28</sup>. It is clearly seen that neither the absolute value (too small compared to the experimental data) nor the temperature dependence (quasi-linear) agrees with the  $H_J(T)$  data. Since the actual penetration field is larger than the thermodynamic  $H_{c1}(T)$ , it is therefore quite natural to assume that a Bean-Livingston surface barrier impedes field penetration, and yields a larger entry field  $H_e^{2D}(T)$ .

In anisotropic superconductors, in the quasi-2D regime, e.g. when the transverse coherence length  $\xi_c$  becomes smaller than the interlayer distance  $d$ ,  $H_e^{2D}(T)$  was shown to be related only to the  $c$ -axis penetration length through<sup>7</sup>:

$$H_e^{2D}(T) = \frac{\phi_0}{4\pi\lambda_c(T)d} \quad (2)$$

In Bi-2212, the quasi-2D regime holds up to temperatures very close to  $T_c$ , so that this last expression for  $H_e^{2D}(T)$  is valid in our measuring temperature range. A surface barrier might thus account for the observed value of the penetration field. Also, since  $H_e^{2D}(T)$  grows as

$1/\lambda_c(T)$  (instead of  $1/\lambda_{ab}\lambda_c(T)$ ), it is expected that the temperature dependence could show a better agreement. The existence of a surface barrier is further suggested by the hysteretic behavior of dissipation, shown in Fig. 4, at  $T = 65$  K (the behavior is similar at other temperatures). When the field is swept down, vortices do not exit in a reversible way. However all vortices have left the sample as can be inferred from the recovery of the same dissipation as in zero initial field, when the field is back to zero value. When the field is swept up again, the absorption displays precisely the same behavior as after the zero field cooled procedure. Bulk pinning would induce flux trapping at zero field, hence some residual dissipation. Our observations are similar to magnetization measurements where the irreversibility, assigned to a surface barrier, is characterised by zero magnetization upon decreasing field. Such a behavior, first observed in a field parallel to the  $c$ -axis<sup>44</sup>, was also reported for Josephson vortices in Bi-2212 in a field oriented nearly parallel to the  $ab$  plane<sup>38</sup>. Surface barriers may also lead to time dependent effects<sup>45</sup>. Indeed, it was argued from magnetization data taken at various sweep rates that the penetration field in the parallel configuration depends on the field sweep rate, and eventually achieves the thermodynamic first critical field value for the slowest rates<sup>10</sup>. Our sweeping rate is of the order of 0.1 Oe/s, comparable to the range where the largest penetration fields were observed<sup>10</sup>. We did not change the sweeping rate hence we cannot confirm this claim. We point out however that the penetration fields observed in<sup>10</sup> are significantly smaller (roughly a factor of 3) than ours. Compared to the fastest rate, the decrease of the penetration field associated to the slowest rate is only 1 Oe. Such small values can obviously be more easily reconciled with  $H_{c1}(T)$  than ours.

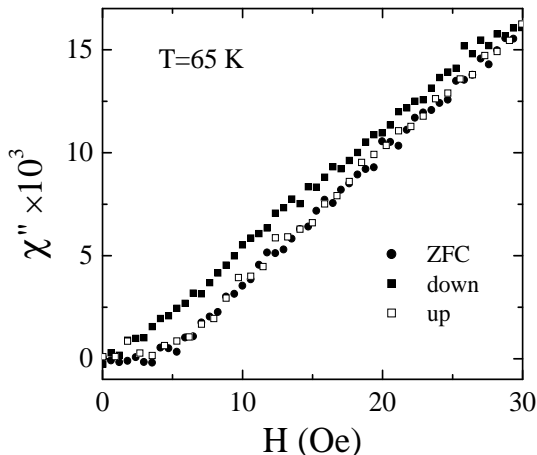


FIG. 4. Plot of  $\chi''(H)$  as a function of the direction of the field sweep. Full circles, full squares and open squares refer to sweeping up the field starting from a ZFC state, sweeping down the field to zero, and sweeping up the field again respectively.

It is worth noting that all these remarks do not modify

the surface barrier interpretation: they only put a time scale for its observation.

Relying on the results described above, we derive from the  $H_J(T)$  data an effective penetration depth  $\lambda_J(T)$  using Eq. (2). The data are shown in Fig. 5. We then try to determine  $\lambda_c(0)$  so as to fit  $\lambda_J(T)$  using the measured  $\Delta\lambda_c(T)$ . We find that both sets of data, namely  $\lambda_J(T)$  and  $\Delta\lambda_c(T)$  cannot be reconciled for any value we may assume for  $\lambda_c(0)$ . Therefore, the interpretation cannot be so simple.

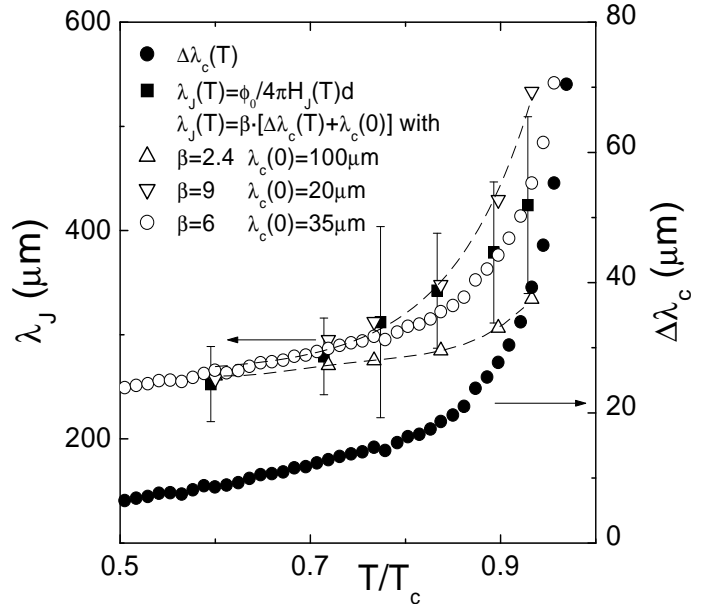


FIG. 5. Plot of the temperature variation  $\Delta\lambda_c(T)$  (full circles, right scale) and of the effective length  $\lambda_J(T)$  which is associated to a surface barrier for the penetration of Josephson vortices (full squares, left scale), using Eq. (19) or (21). Open circles display the best fit using  $\lambda_c(0) = 35 \mu\text{m}$  and a scaling factor  $\beta = 6$ . Open symbols show the best fits using  $\lambda_c(0) = 20 \mu\text{m}$  (down triangles) and  $\lambda_c(0) = 100 \mu\text{m}$  (up triangles).

## V. ROLE OF SURFACE IRREGULARITIES

### A. Experimental checks

Actually, a surface barrier is only effective if the surface is smooth on a typical length scale which is the penetration depth. In our field geometry, defects either located on the top and bottom, e.g.  $ab$ -planes, or the edges may destroy the surface barrier. In the former case, the relevant length scale is  $\lambda_{ab}(T)$ , in the latter case,  $\lambda_c(T)$ .

In order to distinguish between these two possibilities, we have carried out several checks. The samples discussed in this paper were first measured without any special preparation except for their initial shaping in platelet and cleaving in order to work on a well defined single crystal and mirror-like surfaces. We noticed that cleaved

surfaces often exhibit a few visible steps and sparse voids. After the first measurement, sample D was placed on the stage of an STM and the tip was used in order to cut four grooves parallel to the small side of the crystal, 4000 Å deep and 100 μm apart. Then the sample was measured again ( $\mathbf{H}$  parallel to the grooves). No significant change in the onset field of the microwave absorption was observed. In a second step, we took another sample yielding a similar penetration field, and cleaved it. We obtained fresh surfaces with one or two isolated steps which could be seen under a binocular. This sample was measured immediately after cleaving, and again, no significant change was observed. It seems therefore that either defects within the  $ab$ -planes do not play any role in order to reduce a surface barrier or even a single step is immediately effective to destroy the surface barrier.

One should also consider penetration through the edges. Indeed, the edges are fairly difficult to control. We did check indirectly, in the surface impedance and ac-susceptibility experiments, whether they play any role. In order to measure  $\Delta\lambda_c(T)$ , the rf magnetic field applied parallel to the plane is also parallel to one edge of the crystal. If the sample is rotated by 90° along its  $c$ -axis, the edges where  $c$ -axis currents flow are interchanged. It is then clear that if there exists a large defect, e.g. a slit or groove deep in one edge and not in the other, this defect changes significantly the  $c$ -axis microwave current pattern in one position and much less in the other. Therefore, the two configurations should yield a different  $\Delta\lambda_c(T)$  result. In one particular sample out of three, this was indeed the case, suggesting the presence of a defect lying in one edge and showing that the measured  $\Delta\lambda_c(T)$  cannot be intrinsic for this particular sample. The data used in this paper and shown in Fig. 5 are not biased by such large edge defects, e.g. the  $\Delta\lambda_c(T)$  data displayed in Fig. 5 are unchanged within the accuracy of the measurement upon this rotation.

We have now to examine quantitatively to which extent defects located on the top or bottom surfaces, or in the edges alter the penetration field.

## B. Theoretical calculations: formalism

As usual the entrance field is deduced from the balance between the vortex attraction to the surface and the pushing force exerted by the screening current at the minimum distance  $\xi$  (the vortex core size)<sup>6,46</sup>. The presence of the surface irregularities can strongly influence the screening current distribution. In particular, near a scratch the current density can be many times larger than near the flat surface. This may substantially increase the force pushing vortices inside the superconductor and then decrease the surface barrier and the entrance field. The vortex attraction to the surface does not change essentially near a scratch, as it has been demonstrated in Ref.<sup>47</sup>. The force of attraction can decrease by at most a

factor of two near the defect. Then, the main change of the entrance field is essentially related with the increase of the screening current density.

We consider the case where the scratch is in the form of a groove on the superconductor surface, and the magnetic field is parallel to it. Let the  $z$ -axis be perpendicular to the superconductor surface. The magnetic field is parallel to this surface along the  $y$ -axis, and we choose the axis of the groove on the same direction. The depth of the scratch is denoted as  $b$  and its width  $2a$  (see Fig. 6). For convenience, the semi-axis  $z > 0$ , is chosen inside the superconducting material, so in Fig. 6 the scratch is presented on the bottom surface of the superconductor. Both  $a$  and  $b$  are supposed to be much smaller than  $\lambda$ , the London penetration depth, so screening can be ignored and the two-dimensional London equation reduces to Poisson's equation. Then the lines of current correspond to the equipotentials, and a dielectric defect in a superconductor corresponds to a metallic embedding in electrostatics<sup>48</sup>. This analogy reduces our problem to the calculation of the electric field distribution near a metallic electrode having the special form (Fig. 6) while the field becomes uniform for  $z \rightarrow \infty$ . As is known from electrostatics (see, e.g., Ref.<sup>49</sup>), the solution is provided by a conformal transformation of the  $w$ -plane, corresponding to a flat surface, to the  $\zeta$ -plane, the plane of an orthogonal cut of the scratch. In the  $w$ -plane the attraction energy of the plane on a vortex located at the point  $w$  can be easily computed, for example by the image method<sup>46</sup>

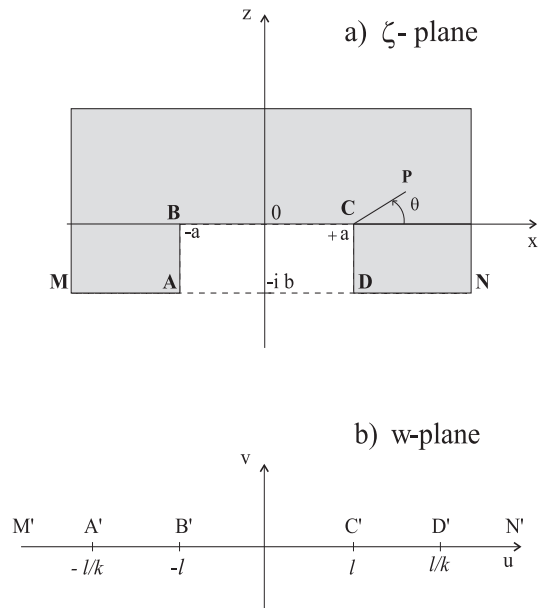


FIG. 6. a) The defect MABCDN in the form of the groove at the bottom surface of superconductor. The plane of the figure corresponds to the plane  $\zeta = x + iz$ . b) The plane  $w = u + iv$  where the straight line  $M'A'B'C'D'N'$  is mapped to the surface line MABCDN.

$$E_{att}(w) = - \left( \frac{\phi_0}{4\pi\lambda} \right)^2 \ln \frac{\lambda}{w - \bar{w}}. \quad (3)$$

Besides, a uniform current density  $j(w) = j_0$  in the  $w$ -plane, can be deduced from the simple complex potential  $\psi(w) = j_0 w$ . Then in the  $\zeta$ -plane, the complex current density  $j(\zeta)$  can be obtained from the complex potential  $\psi(\zeta) = j_0 w(\zeta)$  by

$$j(\zeta) = \frac{d\psi}{d\zeta} = j_0 \frac{dw(\zeta)}{d\zeta}, \quad (4)$$

where  $j_0$  is the current density far away from the defect, i.e., the screening current near the surface  $j_0 = cH/4\pi\lambda$ . To calculate both the attraction energy and the current density in the  $\zeta$ -plane, we need to inverse the conformal transformation. In general, this cannot be done analytically. However, for situations of practical interest, we may use approximations that allow us to obtain an analytic solution.

### C. Isotropic case

In the Appendix, we have demonstrated that according the values of  $a, b, \zeta$ , there are three different regimes:

- (i)  $a \ll b \sim |\zeta|$  slit-like defect,
- (ii)  $|\zeta| \ll a \ll b$  groove-like defect,
- (iii)  $|\zeta| \ll b \ll a$  step-like defect.

Let us begin by the slit-like defect. In this case, we use equations (A9) and (A12) to derive the vortex attraction energy at the distance  $z$  from the slit

$$E_{att}(z) = - \left( \frac{\phi_0}{4\pi\lambda} \right)^2 \ln \frac{\lambda}{2\sqrt{2bz}}, \quad (5)$$

and the strength of the attraction force is

$$f_{att}(z) = \frac{1}{2} \left( \frac{\phi_0}{4\pi\lambda} \right)^2 \frac{1}{z}, \quad (6)$$

that is half of the force for a plane surface. Similarly the current density is

$$j(z) = \frac{1}{\sqrt{2}} j_0 \sqrt{\frac{b}{z}}. \quad (7)$$

These two results were obtained earlier<sup>47</sup> for the field and current distribution near the angle  $2\pi$  (the cut at the superconductor surface).

The balance between the vortex attraction to the surface and the pushing force exerted by the screening current at the minimum distance  $\xi$  (the vortex core size)<sup>6,46</sup> gives the entrance field near the defect

$$H_{ed} \simeq H_e \left( \frac{\xi}{b} \right)^{1/2}, \quad (8)$$

where  $H_e$  is the entrance field for the flat surface  $H_e \simeq \phi_0/4\pi\lambda\xi \simeq H_c$  (thermodynamic critical field). The current concentration effect near the slit essentially reduces

the entrance field. In fact this situation where  $z \sim \xi \gg a$  is not realistic for isotropic superconductors, but it will be useful for the description of the anisotropic ones.

For the groove-like defect, equations (A14) and (A16) allow to derive the physical quantities in the vicinity of the point  $C$ . Let  $P$  be a point such that

$$\zeta_P = a + \rho e^{i\theta}, \quad \rho \ll a. \quad (9)$$

The values of  $\theta$  are limited by the groove and the core of the vortex

$$-\frac{\pi}{2} + \arcsin(\xi/\rho) \leq \theta \leq \pi - \arcsin(\xi/\rho). \quad (10)$$

The attraction energy on a vortex at the point  $P$  is

$$E_{att}(\rho, \theta) = - \left( \frac{\phi_0}{4\pi\lambda} \right)^2 \ln \left[ \left( \frac{2}{9b\rho^2\sqrt{\pi}} \right)^{1/3} \frac{\lambda}{\sin(\frac{2\theta+\pi}{3})} \right], \quad (11)$$

and the strength of the attraction force reads

$$f_{att}(\rho, \theta) = \frac{2}{3} \left( \frac{\phi_0}{4\pi\lambda} \right)^2 \frac{1}{\rho \sin(\frac{2\theta+\pi}{3})}. \quad (12)$$

Its maximum is obtained for  $\theta = 0$  or  $\pi/2$ , this strength is reduced by a factor  $4/(3\sqrt{3}) \simeq 0.77$  by comparing to a flat surface. The calculation of the current density at the point  $P$  gives

$$j(z) = \left( \frac{\sqrt{\pi}}{6} \right)^{1/3} j_0 \left( \frac{b}{a} \right)^{1/6} \left( \frac{b}{\rho} \right)^{1/3} e^{-i\theta/3}. \quad (13)$$

As usual by setting a vortex at a distance  $\xi$  near the defect, we obtain for the entrance field

$$H_{ed} \simeq 2 \left( \frac{2}{9\sqrt{\pi}} \right)^{1/3} H_e \left( \frac{a}{b} \right)^{1/6} \left( \frac{\xi}{b} \right)^{1/3}, \quad (14)$$

where  $[16/(9\sqrt{\pi})]^{1/3} \simeq 1$ .

Finally, for a step  $a \gg b$ , by using equations (A14) and (A17) we can derive the vortex attraction energy and the current density at the point  $P$  in the vicinity of the point  $C$ . The vortex attraction force is still given by Eq. (12) while the current distribution near the corner becomes

$$j(\rho, \theta) \simeq \left( \frac{4}{3\pi} \right)^{1/3} j_0 \left( \frac{b}{\rho} \right)^{1/3} e^{-i\theta/3}. \quad (15)$$

The corresponding entrance field is

$$H_{ed} \simeq \left( \frac{2\pi}{9} \right)^{1/3} H_e \left( \frac{\xi}{b} \right)^{1/3}, \quad (16)$$

where  $(2\pi/9)^{1/3} \simeq 0.89$ .

### D. Anisotropic case

Now we consider the case of anisotropic superconductors, keeping in mind layered high- $T_c$  materials. As usual, let the  $z$ -axis (or  $c$ -axis) be perpendicular to the superconducting layers. We shall consider two cases : either the groove is on the bottom surface of the crystal, or it is on the side surface (edge) of the layered material. In both cases we choose the axis of the groove parallel to the layers along the  $y$ -axis, and the magnetic field in the same direction :  $\mathbf{h} = h(x,z) \mathbf{e}_y$ . For such a geometry we may write the London free energy of the anisotropic superconductor as

$$F = \frac{1}{8\pi} \int \left[ h^2 + \lambda_{ab}^2 \left( \frac{\partial h}{\partial x} \right)^2 + \lambda_c^2 \left( \frac{\partial h}{\partial z} \right)^2 \right] dV, \quad (17)$$

where  $\lambda_c$  is the London penetration depth when the screening current is flowing along the  $z$ -axis ( $c$ -axis) and  $\lambda_{ab}$  when the current is in  $(x, y)$  plane. For a high- $T_c$  superconductor, we have  $\lambda_c \gg \lambda_{ab}$ .

For a very anisotropic superconductor, in the quasi  $2D$  regime we have  $\xi_c < d$ , where  $d$  is the interlayer distance. In such a case, we need to use  $d$  as the size, in the  $z$ -direction, of the vortex core<sup>7</sup> in calculating the entrance field. For the flat surface the entrance field becomes  $H_e^{2D} \simeq \phi_0/[4\pi d\lambda_c]$ .

By making a scaling transformation, we introduce a new coordinate :  $X = (\lambda_{ab}/\lambda_c)x \ll x^{47}$ . Then the London free energy (17) takes the same form as for the isotropic superconductor with the London penetration depth  $\lambda_{ab}$  and we can use the results of the previous section.

Let us consider the case when the groove is on the bottom surface of the crystal. Under the scaling transformation, the width of the groove changes

$$a \rightarrow a' = \frac{\lambda_{ab}}{\lambda_c} a \ll a. \quad (18)$$

Then, the entrance field will be given by the corresponding formulas for the isotropic case with the replacement of  $a$  by  $a'$  and  $\xi$  by  $\xi_c$ , the correlation length along the  $z$ -axis (or by  $d$  when  $\xi_c < d$ ).

For  $d \sim b \gg a'$ , the groove may be considered simply as a thin cut at the surface and by using Eq. (8) we derive

$$H_{ed}^{2D} \simeq H_e^{2D} \left( \frac{d}{b} \right)^{1/2}. \quad (19)$$

Note that due to the large anisotropy of some high- $T_c$  materials, this situation could be realized in practice despite the fact that  $d$  is of the order of only  $10 \text{ \AA}$ .

In the opposite case  $d \ll a' \ll b$ , Eq. (14) gives the entrance field near the groove

$$H_{ed}^{2D} \simeq H_e^{2D} \left( \frac{d}{b} \right)^{1/3} \left( \frac{a\lambda_{ab}}{b\lambda_c} \right)^{1/6}. \quad (20)$$

Near the step  $a' \gg b \gg d$ , the entrance field becomes

$$H_{ed}^{2D} \simeq H_e^{2D} \left( \frac{d}{b} \right)^{1/3}. \quad (21)$$

Finally, if the groove-like scratch is on the side surface of the layered material, its effective depth  $b'$  after the scaling transformation becomes much smaller

$$b' = \frac{\lambda_{ab}}{\lambda_c} b \ll b. \quad (22)$$

Then for  $b' \ll a$  such a scratch has practically no effect on the vortex entrance. In the opposite case  $b' \gg a > d$ , by using Eq. (14), we obtain for the entrance field :

$$H_{ed}^{2D} \simeq H_e^{2D} \left( \frac{d}{b} \right)^{1/3} \left( \frac{a}{b} \right)^{1/6} \left( \frac{\lambda_c}{\lambda_{ab}} \right)^{1/2}. \quad (23)$$

In fact the lateral defect must be rather deep:  $b \gg a\lambda_c/\lambda_{ab} \geq d\lambda_c/\lambda_{ab}$  to strongly reduce the entrance field value. We may deduce that the parallel entrance field depends strongly on the surface defects in layered superconductors. The current concentration near the defect edges may greatly reduce the entrance field in comparison to its theoretical value  $H_e^{2D} \simeq \phi_0/4\pi d\lambda_c$ .

### E. Comparison with experimental data

We have therefore attempted to fit our data derived from  $H_J(T)$  with Eqs. (19), (21) or (23), using two adjustable parameters: a scaling factor  $\beta$  associated with the defect geometry which equals to  $(b/d)^{1/2}$  in Eq. (19),  $(b/d)^{1/3}$  in Eq. (21),  $(d^2 a/b^3)^{1/6}$  in Eq. (23), and the absolute value of  $\lambda_c(0)$ . We show the results in Fig. 5, only for the case described by Eqs. (19) and (21) (defect in the  $ab$ -plane), where we have determined the scaling factor and  $\lambda_c(0)$  which allow to adjust  $\lambda_J(T)$ . We find a best fit for  $\lambda_c(0) = 35 \text{ \mu m}$  and a scaling factor  $\beta = 6$ . Assuming a thin groove, this yields  $b \sim 500 \text{ \AA}$  which is reasonable. We also show in Fig. 5 smaller and larger values for  $\lambda_c(0)$ . They allow us to set the uncertainty about our determination of the penetration depth.

As for Eq. (23) (edge defect), we have taken  $\lambda_{ab}(0) = 2600 \text{ \AA}$ . We can also account for the data but only in a very restricted, nevertheless acceptable, range of parameters. The depth of the edge slit should be of the order of  $10 \text{ \mu m}$ , which is still small with respect to  $\lambda_c(0)$ . The key result in this latter case is that it yields the same absolute value for  $\lambda_c(0)$ .

In conclusion, the set of experiments that we have performed suggest very strongly a surface barrier which impedes field penetration, nevertheless partially destroyed according to the calculations developed in the framework of this work. Although we cannot ascertain which specific defects reduce the efficiency of the surface barrier, we obtain a fairly good estimate of the  $c$ -axis penetration depth.

## VI. ACKNOWLEDGEMENTS

This work was supported by the Centre National de la Recherche Scientifique - Russian Academy of Sciences cooperation program 4985, and by CREST and Grant-in-Aid for Scientific Research from the Ministry of Education, Science, Sports and Culture (Japan). The work at ISSP was also supported by the Russian Fund for Basic Research (grant 00-02-17053) and Scientific Council on Superconductivity (project 96060).

## APPENDIX: CONFORMAL TRANSFORMATION

The Schwarz-Christoffel conformal transformation of the  $w$  plane ( $w = u + iv$ ) to the  $\zeta$  plane ( $\zeta = x + iz$ ) which maps the straight line  $M'A'B'C'D'N'$  (Fig. 6b) to the surface line  $MABCDN$  (Fig. 6a) is<sup>49</sup>

$$\zeta(w) = A \int_0^{w/\ell} \sqrt{\frac{1-t^2}{1-k^2t^2}} dt, \quad (\text{A1})$$

where the two parameters  $k$  and  $\ell$  are related to the dimensions  $a$  and  $b$  of the groove, and the constant  $A$  is simply

$$A^{-1} = a^{-1} \int_0^1 \sqrt{\frac{1-t^2}{1-k^2t^2}} dt. \quad (\text{A2})$$

The integrals of the two previous equations can be expressed in terms of incomplete and complete elliptic integrals  $E(z, k)$ ,  $F(z, k)$ ,  $E(k) \equiv E(1, k)$ ,  $K(k) \equiv F(1, k)$ <sup>50</sup>. For this we define two  $G$  functions, one incomplete and one complete as :

$$\begin{aligned} G(z, k) &= E(z, k) - k'^2 F(z, k), \\ G(k) &= G(1, k) = E(k) - k'^2 K(k), \end{aligned} \quad (\text{A3})$$

where  $k' = \sqrt{1-k^2}$ . Then the conformal transformation reads

$$\zeta(w) = a \frac{G(w/\ell, k)}{G(k)}. \quad (\text{A4})$$

The dimensionless parameter  $k \in [0, 1]$  is determined by the following equation,

$$\frac{a}{b} = \frac{G(k)}{G(k')}. \quad (\text{A5})$$

The limits  $k \rightarrow 0$  and  $k \rightarrow 1$  correspond to  $a/b \rightarrow 0$  and  $a/b \rightarrow \infty$  respectively. The last parameter  $\ell$ , the dimension of which is a length, is determined by requiring that at a large distance from the defect, the two variables  $\zeta$  and  $w$  become equal. Using the asymptotic form of  $G(z, k)$  for large  $z$ ,

$$|z| \gg 1/k \Rightarrow G(z, k) \simeq kz, \quad (\text{A6})$$

we get

$$\ell = a \frac{k}{G(k)}. \quad (\text{A7})$$

When  $k \rightarrow 0$ , i.e.,  $k' \rightarrow 1$ , the following asymptotic forms of the elliptic integrals

$$k \rightarrow 0, \quad G(k) \simeq \frac{\pi}{4} k^2, \quad G(k') \simeq 1, \quad (\text{A8})$$

may be used to determine the parameters  $k$  and  $\ell$  in the limits  $a/b \rightarrow 0$  or  $a/b \rightarrow \infty$

$$a/b \rightarrow 0, \quad k \simeq \frac{2}{\sqrt{\pi}} \sqrt{\frac{a}{b}}, \quad \ell \simeq \frac{2}{\sqrt{\pi}} \sqrt{ab}, \quad (\text{A9})$$

$$a/b \rightarrow \infty, \quad k \simeq 1 - \frac{2b}{\pi a}, \quad \ell \simeq a. \quad (\text{A10})$$

Firstly, we suppose that the groove is very narrow  $a \ll b$ , and we consider the region where  $\zeta \sim w \sim b$ . Then we have  $|w| \gg \ell$  and the elliptic integrals can be approximated as

$$k \rightarrow 0, 1 \ll |z| \ll 1/k \Rightarrow G(z, k) \simeq \frac{i}{2} k^2 z^2. \quad (\text{A11})$$

The conformal transformation becomes simpler and it can be inverted

$$\zeta(w) = \frac{i}{2} \frac{w^2}{b} \Leftrightarrow w(\zeta) = e^{i\pi/4} \sqrt{2b} w^{1/2}. \quad (\text{A12})$$

Secondly we consider the vicinity of the point  $C$  in the  $\zeta$ -plane ( $|\zeta - a| \ll a$ ) and of  $C'$  in the  $w$ -plane ( $|w - \ell| \ll \ell$ ). In this case we have  $|w/\ell - 1| \ll 1$  and the behaviour of the elliptic integrals is

$$|\eta| \ll 1 \Rightarrow G(1 + \eta, k) \simeq G(k) - i \frac{2\sqrt{2}k^2}{3k'} \eta^{3/2}. \quad (\text{A13})$$

As previously the conformal transformation can be easily inverted

$$\begin{aligned} \zeta(w) - a &\simeq \frac{i}{\sqrt{a}} \left( \frac{w - \ell}{\varphi(k)} \right)^{3/2} \Leftrightarrow \\ w(\zeta) - \ell &= e^{i\pi/3} \varphi(k) a^{1/3} (\zeta - a)^{2/3}, \end{aligned} \quad (\text{A14})$$

where the function  $\varphi(k)$  is defined as

$$\varphi(k) = \frac{1}{2} \left[ \frac{9k'^2}{kG(k)} \right]^{1/3}. \quad (\text{A15})$$

The asymptotic forms of this function read

$$a/b \rightarrow 0, \quad \varphi(k) \simeq \frac{1}{2} \left( \frac{9\sqrt{\pi}}{2} \right)^{1/3} \sqrt{\frac{b}{a}}, \quad (\text{A16})$$

$$a/b \rightarrow \infty, \quad \varphi(k) \simeq \left( \frac{9}{2\pi} \right)^{1/3} \left( \frac{b}{a} \right). \quad (\text{A17})$$

Note that in this last limit  $a \gg b$ , we retrieve the case of a single step defect. The second step at the point  $C$  is not involved.

- <sup>1</sup> W. Lawrence and S. Doniach, Proceedings of the 12th International Conference on Low Temperature Physics, Kyoto, Japan, ed. by E.Kanda, p.361 (1971).
- <sup>2</sup> J.R. Clem and M.W. Coffey, Phys. Rev. B **42**, 6209 (1990).
- <sup>3</sup> J.R. Clem, M.W. Coffey, and Z. Hao, Phys. Rev. B **44**, 2732 (1991).
- <sup>4</sup> R. Kleiner, F. Steinmeyer, G. Kunkel, and P. Müller, Phys. Rev. Lett. **68**, 2394 (1992); R. Kleiner and P. Müller, Phys. Rev. B **49**, 1327 (1994); K. Schlenga, R. Kleiner, G. Hechtfisher, M. Mössle, S. Scmitt, P. Müller, Ch. Helm, Ch. Preis, F. Forsthofer, J. Keller, H.L. Johnson, M. Veith, and E. Steinbeiss, Phys. Rev. B **57**, 14518 (1998).
- <sup>5</sup> P.W. Anderson, Science **268**, 1154 (1995).
- <sup>6</sup> C.P. Bean and J.B. Livingston, Phys. Rev. Lett. **12**, 14 (1964).
- <sup>7</sup> A. Buzdin and D. Feinberg, Phys. Lett. **A165**, 281 (1992).
- <sup>8</sup> F. Zuo, S. Khizroev, X. Jiang, J.L. Peng, and R.L. Greene, Phys. Rev. Lett. **72**, 1746 (1994).
- <sup>9</sup> F. Zuo and S. Khizroev, S. Voss, and A.M. Hermann, Phys. Rev. B **49**, 9252 (1994).
- <sup>10</sup> M. Niderost, R. Frassanito, M. Saalfrank, A.C. Mota, G. Blatter, V.N. Zavaritsky, T.W. Li, and P.H. Kes, Phys. Rev. Lett. **81**, 3231 (1998).
- <sup>11</sup> N.E. Hussey, A. Carrington, J.R. Cooper, and D.C. Sinclair, Phys. Rev. B **50**, 13073 (1994).
- <sup>12</sup> L.N. Bulaevskii, V.L. Pokrovsky, and M.P. Maley, Phys. Rev. Lett. **76**, 1719 (1996).
- <sup>13</sup> A.E. Koshelev, Phys. Rev. Lett. **76**, 1340 (1996).
- <sup>14</sup> Y. Matsuda, M.B. Gaifullin, K. Kumagai, K. Kadowaki, T. Mochiku, and K. Hirata, Phys. Rev. B **55**, R8685 (1997).
- <sup>15</sup> E. Sonin, Phys. Rev. B **60**, 15430 (1999).
- <sup>16</sup> Y. DeWilde, H. Enriquez, N. Bontemps, and T. Tamegai (submitted).
- <sup>17</sup> K. Tamasaku, Y. Nakamura, and S. Uchida, Phys. Rev. Lett. **69**, 1455 (1992).
- <sup>18</sup> C.C. Homes, T. Timusk, R. Liang, D.A. Bonn, and W.N. Hardy, Phys. Rev. Lett. **71**, 1645 (1993).
- <sup>19</sup> D.D. Dulic, D. van der Marel, A.A. Tsvetkov, W.N. Hardy, Z.F. Ren, J.H. Wang, and B.A. Willemsen, Phys. Rev. B **60**, R15051 (1999).
- <sup>20</sup> M.B. Gaifullin, Y. Matsuda, N. Chikumoto, J. Shimoyama, K. Kishio, and R. Yoshizaki, Phys. Rev. Lett. **83**, 3928 (1999).
- <sup>21</sup> Y. Matsuda, M.B. Gaifullin, K. Kumagai, K. Kadowaki, and T. Mochiku, Phys. Rev. Lett. **75**, 4512 (1995).
- <sup>22</sup> T. Tamegai, M. Sato, A. Mashio, T. Shibauchi, and S. Ooi, Proceedings of the 9th International Symposium on Superconductivity, Advances in Superconductivity IX, Ed. S. Nakajima and M. Murakami, 621, Springer-Verlag Tokyo (1997).
- <sup>23</sup> Y. Matsuda, M. Gaifullin, K. Kumagai, M. Kosugi, and K. Hirata, Phys. Rev. Lett. **8**, 1972 (1997).
- <sup>24</sup> E. Sonin, Phys. Rev. Lett. **79**, 3732 (1997).
- <sup>25</sup> M.R. Trunin, Physics–Uspekhi, **41**, 843 (1998); J. Superconductivity **11**, 381 (1998).
- <sup>26</sup> D.V. Shovkun, M.R. Trunin, A.A. Zhukov, Yu.A. Nefyodov, H. Enriquez, N. Bontemps, A. Buzdin, M. Daumens, and T. Tamegai, JETP. Lett. **71**, 92, 2000.
- <sup>27</sup> N. Bontemps, H. Enriquez, and Y. DeWilde, Physics and Materials Science of Vortex states, Flux Pinning and Dynamics, NATO Science Series 356 Ed. R. Kossovsky, S. Bose, W. Pan, and Z. Durusoy 387 (1999).
- <sup>28</sup> T. Jacobs, S. Sridhar, Q. Li, G.D. Gu, and N. Koshizuka, Phys. Rev. Lett. **75**, 4516 (1995).
- <sup>29</sup> S-F. Lee, D.C. Morgan, R.J. Ormeno, D.M. Broun, R.A. Doyle, and J.R. Waldram, Phys. Rev. Lett. **77**, 735 (1996).
- <sup>30</sup> T. Shibauchi, N. Katase, T. Tamegai, and K. Uchinokura, Physica C **264**, 227 (1996).
- <sup>31</sup> J.Le Cohec, G. Lamura, A. Gauzzi, F. Licci, A. Revcolevschi, A. Erb, G. Deutscher, and J. Bok, condmat/0001045 5 Jan 2000.
- <sup>32</sup> H. Enriquez, N. Bontemps, P. Fournier, A. Kapitulnik, A. Maignan and A. Ruyter, Phys. Rev. B **53**, R14757 (1996).
- <sup>33</sup> H. Enriquez, Y. DeWilde, N. Bontemps, and T. Tamegai, Phys. Rev. B **58**, R14745 (1998).
- <sup>34</sup> It might appear attractive to take advantage of the linear, temperature independent, field variation of  $\chi''$  in order to extrapolate the field value for zero dissipation. However, a closer look at the data show that the shape of  $\chi''$  at the onset is temperature dependent and the onset field is found either above or below the extrapolated field. This shows that in the absence of a quantitative understanding of how the dissipation of Josephson vortices sets in, this linear extrapolation remains speculative.
- <sup>35</sup> A. Schilling, F. Hulliger, and H.T. Ott, Z. Phys. B **82**, 9 (1991).
- <sup>36</sup> D.E. Farrell, S. Bonham, J. Foster, Y.C. Chang, P.Z. Jiang, K.G. Vandervoot, D.J. Lam, and V.G. Kogan, Phys. Rev. Lett. **63**, 782 (1989).
- <sup>37</sup> K. Okuda, S. Kawamata, S. Noguchi, N. Itoh, and K. Kadowaki, J. Phys. Soc. Jpn. **60**, 3226 (1991).
- <sup>38</sup> N. Nakamura, G.D. Gu, and N. Koshizuka, Phys. Rev. Lett. **71**, 915 (1993).
- <sup>39</sup> J.C. Martinez, S.H. Brongersma, A. Koshelev, B. Ivlev, P. Kes, R.P. Griessen, D.G. de Groot, Z. Tarnavski, and A.A. Menovsky, Phys. Rev. Lett. **69**, 2276 (1992).
- <sup>40</sup> F. Steinmeyer, R. Kleiner, P. Müller, H. Müller, and K. Winzer, Europhys. Lett. **25**, 459 (1994).
- <sup>41</sup> Y. Iye, I. Oguro, T. Tamegai, W.R. Datars, N. Motohira, and K. Kitazawa, Physica C **199**, 154 (1992).
- <sup>42</sup> O.K.C. Tsui, N.P. Ong, and J.B. Peterson, Phys. Rev. Lett. **76**, 819 (1996).
- <sup>43</sup> B. Khaykovich, E. Zeldov, D. Majer, T.W. Li, P. Kes, and M. Konczykowski, Phys. Rev. Lett. **76**, 2555 (1996).
- <sup>44</sup> M. Konczykowski, L.I. Burlachkov, Y. Yeshurun, and F. Holtzberg, Phys. Rev. B **43**, 13707 (1991).
- <sup>45</sup> L. Burlachkov, Phys. Rev. B **47**, 8056 (1993).
- <sup>46</sup> P. G. De Gennes, Superconductivity of Metals and Alloys (Benjamin, New York, 1996).
- <sup>47</sup> A. Buzdin and M. Daumens, Physica C **294**, 257 (1998).
- <sup>48</sup> A. Buzdin and M. Daumens, Electrostatic analogies in the problems of vortex-defect interactions, to be published.
- <sup>49</sup> E. Durand, Electrostatique, tome II, (Masson, Paris, 1966).
- <sup>50</sup> M. Abramowitz and I. Stegun, Handbook of Mathematical Functions, p.1046, Dover Publications Inc., New York, (1965).